Available online at www.sciencedirect.com
ScienceDirect
Applied Catalysis B: Environmental 81 (2008) 203–217
APPLIED CATALYSIS B: ENVIRONMENTAL
www.elsevier.com/locate/apcatb

A kinetic model for ammonia selective catalytic reduction over Cu-ZSM-5

Louise Olsson [a,*], Hanna Sjövall [a], Richard J. Blint [b]

[a] *Competence Centre for Catalysis, Chemical Reaction Engineering, Chalmers University of Technology, 412 96 Göteborg, Sweden*
[b] *General Motors R&D Center, Chemical and Environmental Sciences Laboratory, 30500 Mound Road, Warren, MI 48090-9055, United States*

Received 31 August 2007; received in revised form 9 December 2007; accepted 12 December 2007
Available online 23 December 2007

Abstract

Kinetic modeling, in combination with flow reactor experiments, was used in this study for simulating NH_3 selective catalytic reduction (SCR) of NO_x over Cu-ZSM-5. First the mass-transfer in the wash-coat was examined experimentally, by using two monoliths: one with 11 wt.% wash-coat and the other sample with 23 wt.% wash-coat. When the ratio between the total flow rate and the wash-coat amount was kept constant similar results for NO_x conversion and NH_3 slip were obtained, indicating no significant mass-transfer limitations in the wash-coat layer. A broad range of experimental conditions was used when developing the model: ammonia temperature programmed desorption (TPD), NH_3 oxidation, NO oxidation, and NH_3 SCR experiments with different NO-to-NO_2 ratios. 5% water was used in all experiments, since water affects the amount of ammonia stored and also the activity of the catalyst. The kinetic model contains seven reaction steps including these for: ammonia adsorption and desorption, NH_3 oxidation, NO oxidation, standard SCR ($NO + O_2 + NH_3$), rapid SCR ($NO + NO_2 + NH_3$), NO_2 SCR ($NO_2 + NH_3$) and N_2O formation. The model describes all experiments well. The kinetic parameters and 95% linearized confidence regions are given in the paper. The model was validated with six experiments not included in the kinetic parameter estimation. The ammonia concentration was varied from 200 up to 800 ppm using NO only as a NO_x source in the first experiment and 50% NO and 50% NO_2 in the second experiment. The model was also validated with transient experiments at 175 and 350 °C where the NO and NH_3 concentrations were varied stepwise with a duration of 2 min for each step. In addition, two short transient experiments were simulated where the NO_2 and NO levels as well as NO_2-to-NO_x ratio were varied. The model could describe all validation experiments very well.

Keywords: Ammonia selective catalytic reduction; Zeolite; Cu-ZSM-5; Kinetic modeling; Mass-transfer

1. Introduction

Diesel engines and lean burn gasoline engines have better fuel economy compared to stoichiometric gasoline engines. However, the conventional three-way catalyst (TWC) cannot reduce the NO_x efficiently, due to the high oxygen content in the exhaust. It is important to decrease the emissions of NO_x for environmental reasons [1,2].

There are three major techniques for reducing NO_x in lean atmosphere; lean NO_x traps [3,4], selective catalytic reduction using hydrocarbons (HC SCR) [1,5,6] and urea selective catalytic reduction (urea SCR) [7–40]. The focus of this work is NH_3 SCR. The ammonia is produced by the decomposition of urea (NH_2–CO–NH_2) [7,8], which can be summarized by the following reactions:

$$NH_2{-}CO{-}NH \rightarrow NH_3 + HNCO \quad (1)$$

$$HNCO + H_2O \rightarrow NH_3 + CO_2 \quad (2)$$

There are many experimental studies on ammonia/urea SCR over different catalysts [9–27], where vanadia is the most well studied catalyst [9–15]. Zeolites are also extensively studied for this reaction; examples of zeolites that have been experimentally investigated for NH_3 SCR are Cu-ZSM-5 [16–20], Cu-faujasite [21,22], H-ZSM-5 [23,24] Fe-ZSM-5 [25,26] and Fe-zeolite-beta [27]. Rahkamaa-Tolonen et al. [19] investigated

* Corresponding author. Tel.: +46 31 772 4390; fax: +46 31 772 3035.
E-mail address: louise.olsson@chalmers.se (L. Olsson).

0926-3373/$ – see front matter © 2007 Elsevier B.V. All rights reserved.
doi:10.1016/j.apcatb.2007.12.011

Nomenclature

a_j	active site density for reaction j (mol-sites/m^3)
A	pre-exponential factor. Depends on rate expression. (The concentrations in the rates are in mol/m^3 and the rates in unit s^{-1})
A_{tot}	front area of the monolith (m^2)
$c_{g,tot}$	the total concentration in the gas bulk, where the temperature is T_g (mol/m^3)
$c_{s,i}$	the molar concentration of the gas specie i at the catalyst surface (mol/m^3)
$c_{s,tot}$	the total concentration at the catalyst surface, where the temperature is T_s (mol/m^3)
D_h	hydraulic diameter of channel (m)
$D_{i,m}$	binary diffusion coefficient of specie i in the mixture (m^2/s)
E_a	activation energy (J/mol)
k	rate constant. Depends on rate expression. (The concentrations in the rates are in mol/m^3 and the rates in unit s^{-1})
$k_{m,i}$	mass-transfer coefficient for specie i (mol/m^2 s)
nr	number of reactions
P_{tot}	total pressure (Pa)
r_j	reaction rate for reaction j (mol/mol-sites s)
R	gas constant (J/mol K)
Sh	Sherwood number
s_{ij}	stoichiometric coefficient of specie i in reaction j
s_{kj}	stoichiometric coefficient of surface specie k in reaction j
S	surface area per reactor volume (m^{-1})
t	time (s)
T_s	temperature at catalyst surface (K)
w	molar flow rate (mol/s)
$x_{g,i}$	mole fraction of gas specie i
$x_{s,i}$	mole fraction of gas specie i at the surface
z	axial position (m)

Greek symbols

α	constant
θ_k	coverage of component k

several zeolites: hydrogen, copper, iron and silver ion-exchanged ZSM-5, mordenite, beta, ferrierite and Y-zeolites.

There are three SCR reactions described in the literature depending on the NO_x source, the standard SCR using NO, the rapid SCR with NO and NO_2 and NO_2 SCR with NO_2 only:

$$4NH_3 + 4NO + O_2 \rightarrow 4N_2 + 6H_2O \quad (3)$$

$$2NH_3 + NO + NO_2 \rightarrow 2N_2 + 3H_2O \quad (4)$$

$$4NH_3 + 3NO_2 \rightarrow 3.5N_2 + 6H_2O \quad (5)$$

It is observed that about 50% of NO_2 is optimum concentration and this has been seen on several catalysts, including vanadia [28], Cu-ZSM-5 [16] and Fe-ZSM-5 [25]. The "Rapid SCR" reaction describes this property well. Tronconi et al. [15] and Chatterjee et al. [29], have suggested a detailed mechanism of this step on vanadia catalysts. Further, at lower temperatures (<200 °C), the ammonia can react with NO_2 producing ammonium nitrate (NH_4NO_3), which may deposit on the catalyst [30], leading to temporary deactivation. NH_4NO_3 is decomposed, primarily to HNO_3 and NH_3 at higher temperature [28]. The formation of ammonium nitrate on vanadia-based catalysts was studied in detail by Ciardelli et al. [14].

Kinetic modeling has been performed for NH_3 SCR. Global models for the standard SCR ($NH_3 + NO + O_2$) under steady-state conditions are presented for vanadia-based catalysts [10,12,31], Cu-ZSM-5 [20], Cu-faujasite [21], HZSM-5 [23] and chromia on titania [32]. However, there are very few kinetic models that consider the effects of transients and the NO-to-NO_2 ratio. Winkler et al. [33] presented a transient model for SCR on a commercial vanadia/titania catalyst. The rates for the rapid and NO_2 SCR from this work were used by Wurzenberger and Wanker [34] in their model for SCR on vanadia. Further, Wurzenberger and Wanker [34] have multiple reaction rates for the standard NH_3 SCR and NH_3 oxidation (four rates for two reactions), where one reaction step is for the steady-state rate and the other one for transients. Lietti et al. [35] developed a transient kinetic model for the standard SCR reaction over vanadia. Chatterjee et al. [29] presents a global kinetic model, with high level of details, for vanadia-based catalysts. The model can adequately describe transients and steady-state conversion and the effect of NO/NO_2 ratio. Further, Malmberg et al. [39] presents a transient model for NH_3 SCR with NO over Fe-zeolite. In a recent study Chatterjee et al. [40] present a transient model over a commercial zeolite, which also includes the rapid SCR reaction.

There are no kinetic models and kinetic parameters published on ammonia SCR over Cu-zeolites, which consider transient experiments and NO-to-NO_2 ratio. The objective of this work is to develop a kinetic model for Cu-ZSM-5. The influence of NO-to-NO_2 ratio was investigated and all experiments contained 5% H_2O. The model considers ammonia adsorption and desorption, NH_3 oxidation, NO oxidation, standard SCR, rapid SCR, NO_2 SCR and N_2O formation. The model is validated with separate experiments not included in the fitting procedure where the ammonia concentration was varied and also four experiments containing short transients. The model can describe these validation experiments well.

2. Experimental

2.1. Catalyst preparation and characterization

All four monolith coated catalysts used in this study were prepared using H-ZSM-5 powder acquired from Alsi-Penta. Details about the ion-exchange and preparation can be found in Ref. [16]. The initial material was H-ZSM-5 with a SiO_2/Al_2O_3 ratio of 27. The zeolite was first ion-exchanged with sodium, using $NaNO_3$, in order to get a more controlled ion-exchange. This was followed by ion-exchange with copper ($Cu(CH_3COO)_2$). The cordierite monoliths had a cell density of 400 cpsi

and consisted of 188 channels. They were first wash-coated with a thin layer of alumina, using 5% boehmite (Disperal D) in a liquid phase of 50% destilled water and 50% ethanol. This was done in order to facilitate the attachment of the zeolite to the monoliths. The incipient wetness impregnation method was also used for applying the zeolite to the monoliths. The solid phase of the slurry contained 80% Cu-ZSM-5 and 20% Boehmite (Disperal D) and the liquid phase consisted of 50% distilled water and 50% ethanol. Cat. 1a and Cat. 1b were prepared at the same time, using the same slurries. The liquid/solid weight ratios in these slurries were 80/20 and 95/5. Cat. 2 and Cat. 3 were prepared later using the same zeolite powder in a slurry, but Cat. 3 had a thinner wash-coat layer (10.6 wt.% wash-coat versus 23.4 wt.% for Cat. 2). Details about the samples are shown in Table 1. A different cordierite substrate was used for Cat. 2 and Cat. 3 compared to Cat. 1a and Cat. 1b, however, both were 400 cpsi. This is the reason for the lower values on the wt.% wash-coat for the samples Cat. 1a and Cat. 1b. The lengths of the monoliths were 30 mm for Cat. 1a and Cat. 1b and 15 mm for Cat. 2 and Cat. 3. The diameters for all samples were 22 mm.

Cat. 1b was characterized and the BET surface area, total pore volume and pore size distribution were measured using a Micromeritics ASAP 2010 instrument. The BET surface area was 304 $m^2/g_{wash\text{-}coat}$ and the total pore volume was 0.226 $cm^3/g_{wash\text{-}coat}$. The pore size distribution was bimodal with two peaks at approximately 40 and 50 Å, where the latter peak has a tailing which levels out at about 100 Å. In addition, there is an increase in the pore volume at about 20 Å, but it is not possible to clearly view the pore sizes from the zeolite since they are very small (pore size openings about 5.5 Å according to the manufacturer, Alsi-Penta). Further, it is not possible to view the macro-pores using this method. The corresponding zeolite powder was also investigated, resulting in a BET surface area of 319 $m^2/g_{wash\text{-}coat}$ and the total pore volume of 0.172 $cm^3/g_{wash\text{-}coat}$.

The copper zeolite was prepared from a H-ZSM-5 powder, which was first ion-exchanged with sodium, as described above. The sodium content was analyzed and was 0.05%, which should be compared with 2.0% Cu. There are 15 times more copper sites in the samples compared to sodium. In addition, we have investigated the SCR activity over Na-ZSM-5 and it had a much lower activity compared to the corresponding Cu-ZSM-5 [16].

2.2. Flow reactor experiments

Details about the reactor system can be found in Ref. [16]. Briefly, it consists of a gas mixing system with nine mass flow controllers (Environics 2000), a reactor and analyzing instruments. The reactor consists of an electrically heated quartz tube, which is 80 cm long and 22 mm in inner diameter. The water was added to the flow using an evaporator at 150 °C. The water concentration was controlled by exerting a pressure with Ar on the water surface in the container. A very thin capillary led the water to the evaporator, in order to produce a pressure drop. Two thermocouples are used to measure the temperature: one placed in the gas phase about 1 cm in front of the catalyst and the second one is situated at the center of the monolith. The thermocouple in the gas phase is used to control the temperature. The temperatures in the monoliths are in most experiments only a few degrees higher than the gas phase temperature and the gradients are at the most 10 °C, except for the NH_3 TPD where the gradient is 20 °C at the highest temperature. The catalyst temperature is used in all simulations, and it is shown in the figures. The NO concentration is measured using a chemiluminescence detector (Eco Physics CLD 700). The NO_2, N_2O and NH_3 are measured with an FTIR (Bio-Rad FTS 3000 Excalibur spectrometer with a Specac Sirocco series heatable gas cell, P/N 24102, with a 2 m pathlength and a volume of 0.19 l).

The inert balance was Ar for all experiments. The catalysts were pre-treated at 500 °C for 20 min using 8% O_2 in Ar, prior to all experiments, in order to clean the surface from residues of NO_x and NH_3.

2.2.1. Experiments for investigating mass-transfer

The mass-transfer in the wash-coat was examined by comparing the results from two catalysts (Cat. 2 and Cat. 3), while keeping the ratio between the flow rate and mass zeolite constant. The total flow rate was 3500 ml/min for the 23% wash-coat sample (Cat. 2) and 1750 ml/min for the 11% wash-coat sample (Cat. 3), respectively. The concentration in these two experiments was 500 ppm NO, 500 ppm NH_3, 8% O_2 and 5% H_2O. The temperature was increased stepwise (values in parentheses refer to reaction time after the specified temperature has been reached): 100 °C (40 min), 150 °C (30 min), 200 °C (30 min), 250 °C (20 min), 300 °C (20 min), 350 °C (20 min), 400 °C (20 min), 450 °C (20 min) and 500 °C (20 min).

2.2.2. Temperature programmed desorption (TPD) and activity measurements

The total flow rate was 3500 ml/min, which corresponds to a space velocity of 18,400 h^{-1}. The ammonia TPD and all activity measurements, except the last two short transients,

Table 1
Details about the catalyst samples used

Sample	Monolith length (mm)	Weight alumina layer (mg)	Weight zeolite layer (mg)	wt.% wash-coat[a]	Cu loading (wt.%) [16]	Ion-exchange level (Cu/Al) [16]
Cat. 1a [16]	30	73	1038	12.2	2.03	0.35
Cat. 1b	30	78	1010	12.7	2.03	0.35
Cat. 2	15	34	496	23.4	2.03	0.35
Cat. 3	15	37	265	10.6	2.03	0.35

[a] Different cordierite monoliths are used for Cat. 1a and Cat. 1b compared to Cat. 2 and Cat. 3.

were performed on Cat. 1a and Cat. 1b. These catalysts (Cat. 1a and Cat. 1b) are prepared at the same time, using the same slurries and they contain very similar amounts of zeolite (1038 and 1010 mg). In addition, after the initial stabilization the samples gave the same conversion (only about 5 ppm difference).

In the ammonia TPD experiment the catalyst (Cat. 1b) was exposed to 500 ppm NH_3 and 5% H_2O for 80 min at 150 °C followed by 60 min of Ar flush. This was followed by a temperature ramp with a heating rate of 10 °C/min up to 500 °C in an Ar environment. The ammonia oxidation was investigated by exposing the catalyst (Cat. 1a) to 500 ppm NH_3, 8% O_2 and 5% H_2O and the temperature was increased stepwise (values in parentheses refer to reaction time after the specified temperature has been reached): 100 °C (50 min), 150 °C (20 min), 200 °C (10 min), 250 °C (10 min), 300 °C (10 min), 350 °C (10 min) and 400 °C (10 min). The NO oxidation was studied on Cat. 1a in a similar experiment, using an inlet gas composition of 500 ppm NO, 8% O_2 and 5% H_2O. The temperature was increased in steps: 100 °C (60 min), 150 °C (20 min), 200 °C (20 min), 250 °C (20 min), 300 °C (20 min), 350 °C (20 min), 400 °C (20 min), 450 °C (20 min) and 500 °C (20 min).

An ammonia SCR experiment was conducted by exposing the catalyst (Cat. 1a) to 500 ppm NH_3, 500 ppm NO, 8% O_2 and 5% H_2O and the temperature was increased stepwise (values in parentheses refer to reaction time after the specified temperature has been reached): 100 °C (40 min), 150 °C (20 min), 200 °C (20 min), 250 °C (20 min), 300 °C (20 min), 350 °C (20 min), 400 °C (20 min), 450 °C (20 min) and 500 °C (20 min).

In two additional experiments the influence of NO/NO_2 ratio was investigated at two different temperatures 175 and 350 °C using Cat. 1b. In these measurements the inlet feed gas was 500 ppm NO_x, 500 ppm NH_3, 8% O_2 and 5% H_2O. The amount of NO_2 was changed 0, 20, 40, 50, 60, 80 and 100% NO_2. At the lower temperature the time duration was 20 min for each ratio except for the first which was 40 min. The time for each step at 350 °C was 15 min.

Two experiments with changing ammonia concentration were used for validation of the model. The temperature was 175 °C for both measurements. In the first experiment Cat. 1a was used and the inlet feed gas was 500 ppm NO, 8% O_2, 5% H_2O and the NH_3 concentration was changed in steps, with 60 min duration: 200, 300, 400, 500, 600, 700 and 800 ppm NH_3. In the second experiment Cat. 1b was used. The gas consisted of 250 ppm NO, 250 ppm NO_2, 8% O_2, 5% H_2O and the ammonia concentration was varied in the same way as for the previous described experiment.

2.2.3. Short transient experiments

Four additional experiments were used for the model validation. The total flow rate was 3500 ml/min, which corresponds to a space velocity of 18,400 h^{-1} for the experiments where Cat. 1a and Cat. 1b are used and 36,800 h^{-1} for Cat. 2. In the first two short transient experiments Cat. 1b was used. The catalyst was first exposed to 500 ppm NO, 500 ppm NH_3, 8% O_2, 5% H_2O for 50 min. Thereafter different concentrations of NO_2 were added in 2 min long pulses while keeping the NO and NH_3 concentrations constant at 500 ppm. This was followed by exposing the catalyst to 500 ppm NO_2, 500 ppm NH_3, 8% O_2, 5% H_2O for 20 min and then pulsing the NO concentration. The inlet concentrations are presented in Fig. 11. In the second experiment the sample was initially exposed to 500 ppm NO, 500 ppm NH_3, 8% O_2, 5% H_2O for 50 min. This was followed by changing the NO_2-to-NO_x ratio in 2 min steps, while keeping the total NO_x and NH_3 levels constant to 500 ppm. The inlet concentrations are displayed in Fig. 12.

In the last two short transient measurements Cat. 2 was used. The catalyst was initially exposed to 500 ppm NO, 500 ppm NH_3, 8% O_2, 5% H_2O for 50 min. The NO was thereafter changed in 2 min sequences and all other gases were remained constant. This was followed by 20 min period of 500 ppm NO, 500 ppm NH_3, 8% O_2, 5% H_2O. Finally, the ammonia concentration was changed in the same way as previously done for NO. In this case the concentrations of all other gases were kept fixed. The inlet concentrations of NO and NH_3 are shown in Figs. 13 and 14. The experiment was performed at 175 and 350 °C.

3. The model

3.1. Mathematical model

Fortran was used to solve the material balances. Since the reaction heat associated with NH_3 SCR is very low it was not included. Further, the catalyst was placed inside the heating zone and we used the measured temperature in the catalyst in the simulations. The catalyst temperature is shown in the figures in Section 4.

The main governing equation for the gas phase species is:

$$\frac{w}{A_{\text{tot}}}\frac{\partial x_{\text{g},i}}{\partial z} = -k_{\text{m},i}S(x_{\text{g},i} - x_{\text{s},i}) = \sum_{j=1}^{\text{nr}} a_j s_{ij} r_j(T_\text{s}, c_\text{s}, \theta) \tag{6}$$

The coverage of component k on the surface is solved by:

$$\frac{\text{d}\theta_k}{\text{d}t} = \sum_{j=1}^{\text{nr}} s_{kj} r_j(T_\text{s}, c_\text{s}, \theta) \tag{7}$$

The relationship between the concentration and the molar fraction is:

$$c_{\text{s},i} = c_{\text{s,tot}} x_{\text{s},i} \tag{8}$$

where

$$c_{\text{s,tot}} = \frac{P_{\text{tot}}}{RT_\text{s}} \tag{9}$$

The film model is used to describe the mass-transfer between the gas and the catalyst surface, which is the middle term in Eq. (6) above. The mass-transfer coefficient was calculated using the Sherwood number ($Sh = 3$):

$$k_{\text{m},i} = \frac{Sh}{D_\text{h}}(c_{\text{g,tot}} D_{i,\text{m}}) \tag{10}$$

The geometric surface area per unit reactor volume, S, in Eq. (6) is given by:

$$\frac{S}{D_h} = 4 \times (\text{cell density}) \quad (11)$$

3.2. The kinetic model

A kinetic model for ammonia SCR was developed. The Arrhenius equation is used to capture the temperature dependence of the rate constants, k:

$$k = Ae^{-E_A/RT_S} \quad (12)$$

The experiments used to develop the model were conducted on Cat. 1a and Cat. 1b. The catalysts were prepared at the same time and using the same slurries. In addition, the samples contained very similar amounts of zeolite (1038 and 1010 mg) and showed the same conversion after the initial stabilization. Therefore, was the same number of active sites used for modeling the experiments over both catalysts.

It is essential to adequately describe the NH_3 adsorption/desorption over a broad temperature range, since this will strongly influence the transient behavior and so a step for adsorption and desorption of ammonia was added. The desorption peak was very broad, thus the ammonia on surface are adsorbed with different energies. Further, calorimetric measurements of ammonia adsorption on HZSM-5 showed that the heat of adsorption varied between 120 and 180 kJ/mol [41]. Thus, ammonia adsorbs both on the copper sites and Brönstedt acid sites. In addition, up to four ammonia molecules can bind to each copper site [42]. In order to make the model as simple as possible, only one adsorption site, denoted S1 was used and the site density was fitted from the ammonia TPD experiment. A coverage dependent activation energy was used for ammonia desorption, which has been used in several other models for this step [13,29,39,40]:

$$E_{1,b} = E_{1,b}(0)(1 - \alpha_1 \theta_{NH_3-S1}) \quad (13)$$

One global rate was added for the ammonia oxidation. In this summary step ammonia on the surface is reacting with oxygen to produce nitrogen and water. To describe the influence of changing the NO/NO_2 ratio is important. However, the catalyst can also oxidize some NO-to-NO_2 on the copper sites and this is described by one reversible step. Since NO oxidation is a reversible reaction and the conversions at higher temperatures are controlled by the thermodynamics the backward rate is determined by the equilibrium constant. The same rate expression for NO oxidation is applied as in our NO_x storage model [3]. The reaction and rate expressions for the above-described processes are shown in Table 2.

Three reaction steps for SCR have been added for the three SCR processes including standard SCR with NO + O_2 (reaction (4)), fast SCR with NO + NO_2 (reaction (5)) and NO_2 SCR with NO_2 (reaction (6)). The reactions and rates are described in Table 3. The standard SCR are described by a rate that includes ammonia on surface and NO in the gas phase. Tronconi et al. [13] also used adsorbed ammonia and gas phase NO in their modeling of ammonia SCR over vanadia and zeolites [40]. Their rate expression also included an inhibition term and the oxygen concentration. Over our copper zeolite we observed only a very small effect of the oxygen concentration, when oxygen is in large excess [16] and we have, therefore, not added it to the model. Further, the inhibition term used by Tronconi et al. [13] was not needed to describe our SCR results on Cu-ZSM-5. This is further discussed below. Our FTIR studies have shown that the rapid SCR can not be explained by reactions between surface species alone and that gas phase NO is likely important [17]. In this model we have, therefore, described the rapid SCR by a reaction between adsorbed ammonia, NO and NO_2. The NO_2 SCR reaction occurs between adsorbed NH_3 and gas phase NO_2 and this reaction is slower than both the standard and rapid SCR reactions. In addition, the N_2O formation is also included in reaction (7). Experimentally, we have observed that the N_2O production increases when increasing the NO_2 concentration, for most conditions. The model describes this with a rate that is proportional to the NO_2 concentration.

Table 2
Reactions and rate expressions for NH_3 adsorption and desorption, NH_3 oxidation and NO oxidation

Reaction number	Reaction	Reaction rate
1	$NH_3 + S1 \overset{r_1}{\longleftrightarrow} NH_3 - S1$	$r_1 = k_{1,f} c_{NH_3} \theta_{S1-vacant} - k_{1,b} \theta_{NH_3-S1}$
2	$2NH_3 - S1 + \frac{3}{2}O_2 \overset{r_2}{\rightarrow} N_2 + 3H_2O + 2S1$	$r_2 = k_2 c_{O_2} \theta_{NH_3-S1}$
3	$NO + \frac{1}{2}O_2 \overset{r_3}{\longleftrightarrow} NO_2$	$r_3 = k_{3,f} c_{O_2}^{1/2} c_{NO} - k_{3,b} c_{NO_2}$ [a]

[a] $k_{3,b}$ is calculated from the thermodynamic restrictions ($\Delta H = 58.279$ kJ/mol and $\Delta S = -76.1$ J/mol K).

Table 3
Reactions and rate expressions for standard SCR with NO+O_2, fast SCR with NO+NO_2, NO_2 SCR and N_2O formation

Reaction number	Reaction	Reaction rate
4	$4NH_3 - S1 + 4NO + O_2 \overset{r_4}{\rightarrow} 4N_2 + 6H_2O + 4S1$	$r_4 = k_4 c_{NO} \theta_{NH_3-S1}$
5	$2NH_3 - S1 + NO + NO_2 \overset{r_5}{\rightarrow} 2N_2 + 3H_2O + 2S1$	$r_5 = k_5 c_{NO} c_{NO_2} \theta_{NH_3-S1}$
6	$4NH_3 - S1 + 3NO_2 \overset{r_6}{\rightarrow} 3.5N_2 + 6H_2O + 4S1$	$r_6 = k_6 c_{NO_2} \theta_{NH_3-S1}$
7	$2NH_3 - S1 + 2NO_2 \overset{r_7}{\rightarrow} N_2 + N_2O + 3H_2O + 2S1$	$r_7 = k_7 c_{NO_2} \theta_{NH_3-S1}$

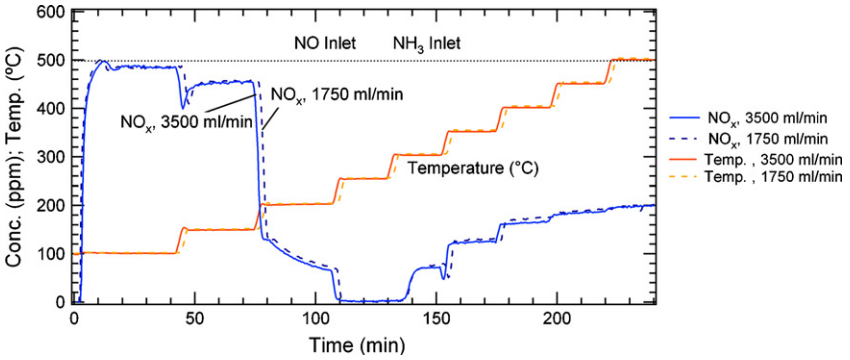

Fig. 1. Comparison of the NO_x concentration for experiments using one monolith with 11% wash-coat and one with 23%. The total flow was 1750 ml/min for the 11% sample and 3500 ml/min for the other sample. The inlet feed gas consisted of 500 ppm NO, 500 ppm NH_3, and 8% O_2.

4. Results and discussion

4.1. Mass-transfer

The mass-transfer in the wash-coat was examined by using two monolith samples, one with 23 wt.% wash-coat (Cat. 2) and the other with 11 wt.% wash-coat (Cat. 3). Both samples were 22 mm in diameter and 15 mm in length. The flow was decreased to 1750 ml/min for the 11% wash-coat (from 3500 ml/min for 23% wash-coat) and this gives the same flow per gram zeolite. The catalyst was exposed to 500 ppm NO, 500 ppm NH_3 and 8% O_2 while increasing the temperature stepwise. Fig. 1 shows a comparison of the measured NO_x out from the catalyst, when using 11 and 23% wash-coat. The temperature is also shown. The corresponding results for the outlet NH_3 concentration are shown in Fig. 2. There is a small difference in time when the temperature increase is started, resulting in a small shift in time for the two curves. The concentrations for the two experiments are very similar. At 300 °C and above the conversion of ammonia is close to 100%, which makes it difficult to draw conclusions regarding mass-transfer limitations at higher temperatures. However, at temperatures below 300 °C the results show that there are no mass-transfer limitations for the standard SCR reaction. The experimental results also show that there are no significant external mass-transfer limitations at temperatures below 300 °C, since the conversion is very similar even though the space velocity is only half for the 11% wash-coat compared to the 23% wash-coat. The experimental observations for the ammonia SCR are discussed for the corresponding experiment on Cat. 1a in Section 4.4. This is done in order to describe the experimental and modeling results simultaneously.

Mass-transport in the wash-coat has been added to some SCR models [36–38], but excluded in some other studies [33,39]. Chatterjee et al. [40] compared ammonia storage, ammonia oxidation and ammonia SCR using a powder and a crushed monolith. They observed a higher SCR activity for the powder even at the lowest temperature measured (200 °C). In addition, the ammonia storage was substantially lower for the crushed monolith and this was observed at 50, 150 and 200 °C. Thus, Chatterjee et al. [40] had mass-transfer limitations in their wash-coat and observed this also at low temperatures. In the first part of our experiment (Fig. 2) there is a total uptake of NH_3 for about 15 min. Both monoliths show the same uptake and also the same conversions. These results indicate that we do not have mass-transport limitations in our wash-coat and we have, therefore, not added this to the model.

4.2. Ammonia storage

The model for ammonia storage and desorption was fitted to one NH_3 TPD experiment, where the catalyst was exposed to 500 ppm NH_3 and 5% H_2O for 80 min at 150°C, followed by 60 min Ar only and finally a temperature ramp. The outlet NH_3

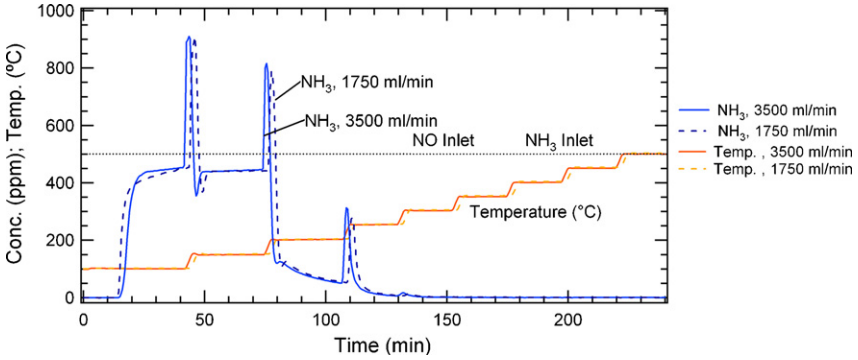

Fig. 2. Comparison of the NH_3 concentration for experiments using one monolith with 11% wash-coat and one with 23%. The total flow was 1750 ml/min for the 11% sample and 3500 ml/min for the other sample. The inlet feed gas consisted of 500 ppm NO, 500 ppm NH_3, and 8% O_2.

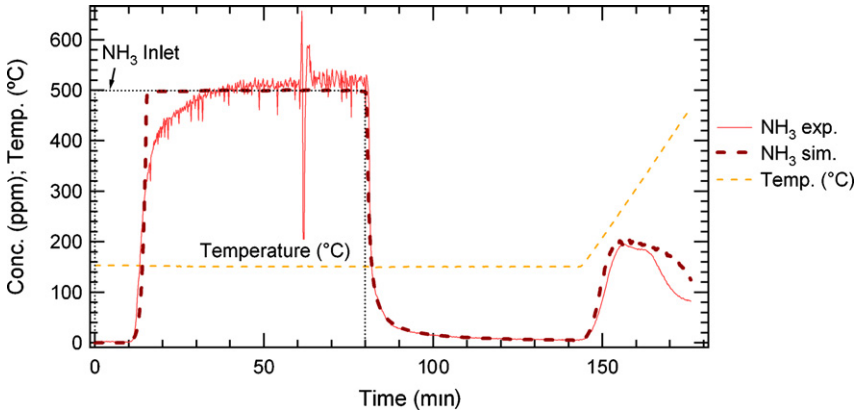

Fig. 3. The measured and calculated outlet NH_3 concentrations during NH_3 TPD experiment are shown, together with the inlet concentration. The catalyst is exposed to 500 ppm NH_3 and 5% H_2O for 80 min at 150 °C followed by Ar only and a temperature ramp. The temperature shown is measured at the centre of the catalyst. The total flow rate is 3500 ml/min.

concentrations from the experiment and simulation are presented in Fig. 3. The spike in ammonia concentration observed experimentally at about 60 min is likely due to an uneven water feed. There is a total uptake of ammonia for about 10 min and thereafter the ammonia concentration starts to increase. The increase is slower experimentally than from the simulation and this might be explained by a slower adsorption when the catalyst is close to saturation. However, this will be of minor importance in the SCR model since the total uptake of ammonia in the model and experiment is very similar. After the ammonia adsorption period the catalyst is exposed to Ar only and desorption of loosely bound ammonia is observed. When increasing the temperature an ammonia desorption peak is seen, with a maximum at about 270 °C. A second peak is observed at about 340 °C; however, there is a large overlap between the peaks. The ramp ends at 480 °C, and at this temperature the desorption of ammonia is not complete. The ammonia concentration is decreasing from the maximum value of 200 ppm to 80 ppm at 480 °C. Thus some of the ammonia is very strongly bound and with this experiment we can observe that ammonia desorbs over a large temperature interval. The temperature was not increased further, because of the risk of sintering the sample in the reducing atmosphere. The model can describe the release of ammonia well, due to the coverage dependent activation energy, which is discussed in Section 3.2. The model also gives ammonia left on the surface at 480 °C, which is in accordance with the experimental observation. The kinetic parameters and their 95% linearized confidence intervals are shown in Table 4. The number of sites was fitted, which resulted in 200.0 ± 2.4 mol-sites/m^3 monolith. This corresponds to 2.75×10^{-3} mol-sites/$g_{zeolite}$ and this result in about seven times more sites compared to copper atoms. Komatsu et al. [42] proposed that four ammonia molecules may coordinate to each copper. Thus, the ammonia in our catalyst is adsorbed on more sites than the copper. As described above it is well known that ammonia also binds to the Brönstedt acid sites [41] and since we have a quite low ion-exchange there are acid sites available in our catalyst, which ammonia can adsorb on. In addition, it is possible that ammonia binds loosely to other sites, since the temperature is quite low. The reason for using only one type of site was to make the model as simple as possible.

4.3. NO oxidation

The Cu-ZSM-5 catalyst has an activity for oxidizing NO-to-NO_2. This is shown in Fig. 4, where the outlet NO and NO_2 concentrations are presented from an experiment where the catalyst was exposed to 500 ppm NO, 8% O_2 and 5% H_2O while stepwise increasing the temperature. The model for the NO oxidation (reaction (3)) was fitted to this experiment and the results from the model are also shown in Fig. 4. At lower temperatures the conversion is kinetically limited and the NO_2 production increases as the temperature increases. The NO_2 reaches its maximum at 450 °C and thereafter starts to decrease due to thermodynamic constraints. The kinetic parameters and their 95% linearized confidence regions are shown in Table 5.

4.4. NH_3 oxidation and ammonia SCR

The ammonia oxidation and ammonia SCR kinetic models were fitted to four experiments. The first experiment was ammonia oxidation, where the catalyst was exposed to 500 ppm NH_3, 8% O_2 and 5% H_2O while increasing the temperature stepwise. The results from experiment and simulation, as well as the inlet NH_3 concentration, are shown in Fig. 5. Initially, there is a large uptake of ammonia and NH_3 breaks through

Table 4
Kinetic parameters for NH_3 storage

Rate	Rate constants	Pre-exponential factor	Activation energy (kJ/mol)	Coverage dependence (α)
NH_3 adsorption ($r_{1,f}$)	$k_{1,f}$	$9.3 \times 10^{-1} \pm 0.2 \times 10^{-1}$	0	–
NH_3 desorption ($r_{1,b}$)	$k_{1,b}$	$1.0 \times 10^{11} \pm 2.2 \times 10^{9}$	181.5 ± 1.3	0.98 ± 0.009

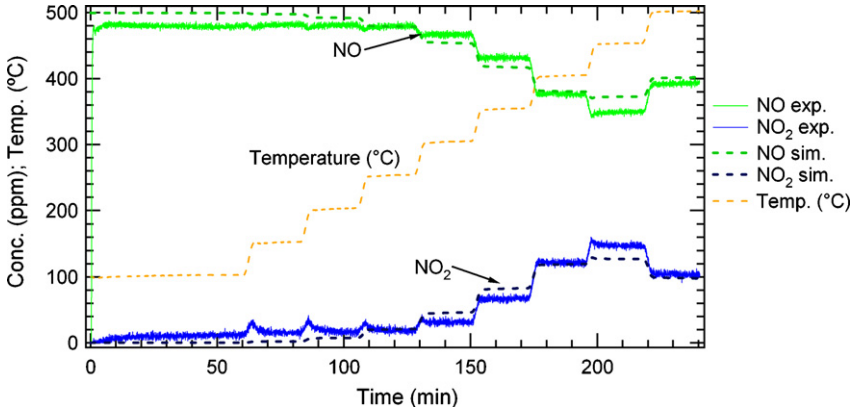

Fig. 4. Measured and calculated concentrations during NO oxidation experiment. The catalyst is exposed to 500 ppm NO, 8% O_2 and 5% H_2O and increasing the temperature stepwise. The temperature shown is measured in the centre of the catalyst. The total flow rate is 3500 ml/min.

Table 5
Kinetic parameters for NO oxidation

Rate	Rate constant	Pre-exponential factor	Activation energy (kJ/mol)
NO oxidation (r_3)	$k_{3,f}$	$8.0 \times 10^1 \pm 0.62 \times 10^1$	48.0 ± 0.41

after about 15 min. There is no ammonia oxidation at this low temperature. Ammonia release is observed when increasing the temperature, due to desorption of ammonia on the catalyst. At 300 °C the ammonia oxidation starts to be significant and increases further when the temperature are increased. The model could describe this experiment adequately.

In the second experiment used in the SCR model development the catalyst was exposed to 500 ppm NO, 500 ppm NH_3, 8% O_2 and 5% H_2O while increasing the temperature stepwise. The results from the experiment and model are shown in Fig. 6. Also in this experiment large ammonia storage is observed initially and when increasing the temperature ammonia desorption is visible. The activity at 100 °C is low. However, already at 150 °C the ammonia SCR increases substantially and at 200 °C the NO conversion is close to 100%. Further, at 150 °C it is observed that the outlet NO and NH_3 concentrations are equal. Thus the stoichiometry is 1:1, which also is used in our model (see Table 6, reaction (4)). This is consistent with other models in the literature over vanadia [13] and zeolites [39,40]. At 350 °C the conversion of NO_x starts to decrease and the concentrations of NO_x now increase gradually when increasing the temperature. This is due to ammonia oxidation, which results in a lower amount of ammonia available for ammonia SCR. This explains the lower conversion at higher temperatures.

The effect of varying the NO/NO_2 ratio (0, 20, 40, 50, 60, 80, 100% NO_2) was investigated at two temperatures, 175 and 350 °C. The concentrations were 500 ppm NO_x, 500 ppm NH_3, 8% O_2 and 5% H_2O. When using a high NO_2 ratio at a low temperature there is a large risk of ammonium nitrate production on the catalyst and in the pipes and detection instruments, which makes the experimental results uncertain. This was seen by Ciardelli et al. [14] who observed large ammonia nitrate formation on the catalyst at 140 °C. At 200 °C there were no deposits onto the catalyst, but there was still a substantial nitrogen loss and they showed that ammonium nitrate was deposited in the reactor system [14]. We, therefore, excluded the 80 and 100% NO_2 case at 175 °C from the simulations. The experimental and simulated NO, NO_2, NH_3 and N_2O concentrations at 175 °C are shown in Fig. 7. During the first 40 min the catalyst was exposed to 500 ppm NO, 500 ppm NH_3, 8% O_2 and 5% H_2O. Initially, the NO concentration out from the catalyst is above 400 ppm and

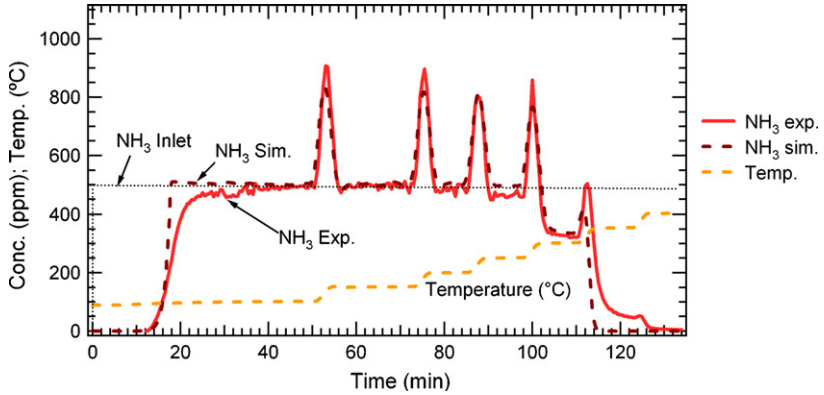

Fig. 5. Measured and calculated concentrations during NH_3 oxidation experiment. The catalyst is exposed to 500 ppm NH_3, 8% O_2 and 5% H_2O while increasing the temperature stepwise. The temperature shown is measured in the centre of the catalyst. The total flow rate is 3500 ml/min.

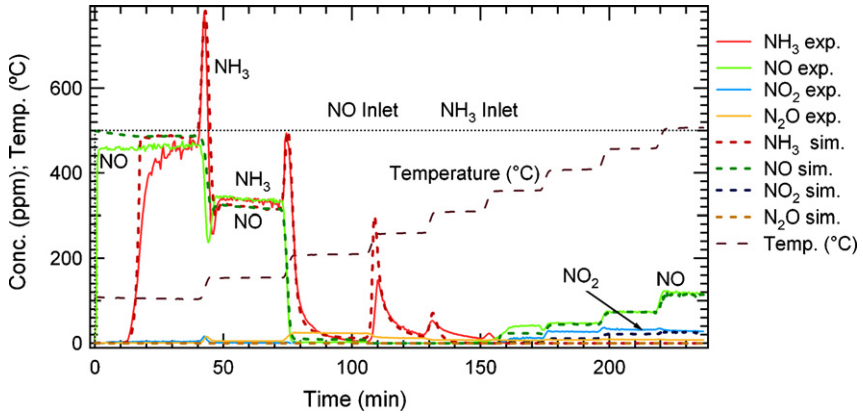

Fig. 6. Measured and calculated concentrations during NH_3 SCR experiment. The catalyst is exposed to 500 ppm NO, 500 ppm NH_3, 8% O_2 and 5% H_2O while increasing the temperature stepwise. The temperature shown is measured in the centre of the catalyst. The total flow rate is 3500 ml/min.

Table 6
Kinetic parameters for NH_3 oxidation and NH_3 SCR

Rate	Rate constants	Pre-exponential factor	Activation energy (kJ/mol)
NH_3 oxidation (r_2)	k_2	$1.2 \times 10^{11} \pm 5.4 \times 10^{8}$	162.4 ± 0.05
Standard SCR, NO + O_2 (r_4)	k_4	$2.3 \times 10^{8} \pm 1.7 \times 10^{6}$	84.9 ± 0.03
Rapid SCR, NO + NO_2 (r_5)	k_5	$1.9 \times 10^{12} \pm 1.6 \times 10^{10}$	85.1 ± 0.3
NO_2 SCR, NO_2 (r_6)	k_6	$1.1 \times 10^{7} \pm 6.8 \times 10^{4}$	72.3 [34]
N_2O formation (r_7)	k_7	$3.6 \times 10^{4} \pm 2.6 \times 10^{2}$	43.3 ± 0.2

the ammonia concentration is zero. Then the NO concentration gradually decreases to a stationary level of about 90 ppm. After slightly more than 20 min the ammonia starts to break. The reason for the long complete uptake is a large storage of ammonia, as described above. In the model the concentration of ammonia on the surface is gradually increasing. The rate for the ammonia SCR reaction is proportional to the coverage of ammonia on the surface (see Table 3, reaction (4)) and thus the rate increases with time, resulting in the observed decrease in NO concentration. The model is able to describe these features well. When increasing the NO_2 content the NO_x conversion increases and reaches a maximum at about 50% NO_2. The conversions are very high and for 40–60% NO_2/NO_x ratio the steady-state levels of both NO and NH_3 are below 30 ppm. The NO_2 concentration is close to zero during the whole experiment. In the model this is explained by the important rapid SCR reaction, between NO, NO_2 and NH_3 (see Table 3, reaction (5)). In addition, when increasing the NO_2 content the N_2O formation is increased. The model describes the N_2O production well, with a rate that depends on the NO_2 concentration.

Fig. 8 shows the corresponding NO_2/NO_x ratio experiment at 350 °C. During the initial 40 min of the experiment the NO_x source is only NO. The conversion of NO is already high. The ammonia slip is zero, which is the case during the whole experiment, due to rapid NH_3 oxidation. Also at this

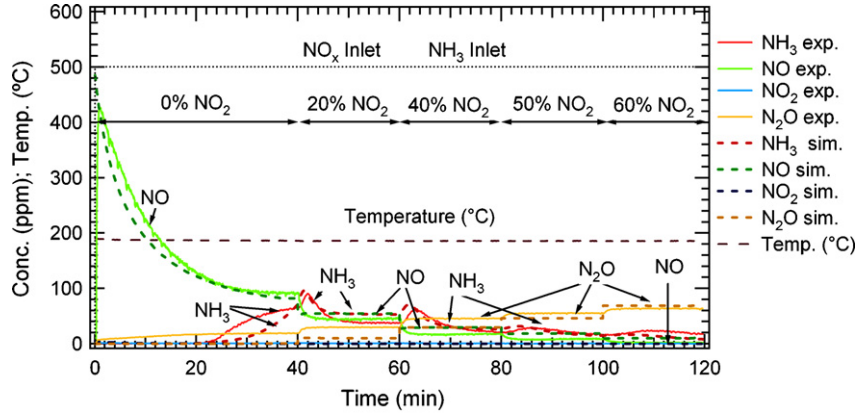

Fig. 7. Measured and calculated concentrations during NH_3 SCR experiment, when varying the NO/NO_2 ratio (0, 20, 40, 50, 60% NO_2). The temperature is 175 °C. The temperature shown is measured in the centre of the catalyst. The total flow rate is 3500 ml/min.

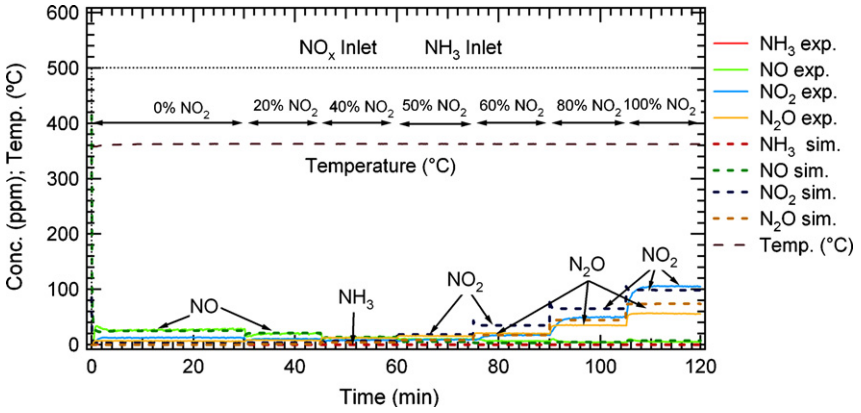

Fig. 8. Measured and calculated concentrations during NH_3 SCR experiment, when varying the NO/NO_2 ratio (0, 20, 40, 50, 60, 80 100% NO_2). The temperature is 350 °C. The temperature shown is measured in the centre of the catalyst. The total flow rate is 3500 ml/min.

temperature the NO_x conversion increases when introducing NO_2 and reaches maximum at about 50% NO_2/NO_x ratio. When increasing the NO_2 fraction further the NO_2 and N_2O concentrations out from the catalyst increases gradually. This is due to the slower NO_2 SCR step and the N_2O step (see Table 3, reactions (6) and (7)). The model can describe the experimental observations well.

The four experiments presented above were used to estimate the kinetic parameters for the NH_3 oxidation and NH_3 SCR. The resulting parameter values and their 95% linearized confidence intervals are shown in Table 6. The activation energy of 162 kJ/mol for ammonia oxidation is very close to the value of 166 kJ/mol Baik et al. [20] obtained over Cu-ZSM-5 and 178 kJ/mol found by Chatterjee et al. [40] over a commercial zeolite. For the standard SCR reaction with NO they obtained lower values, 52 kJ/mol [20] and 49 kJ/mol compared to 85 kJ/mol that we obtained. For the rapid SCR we found a value of 85 kJ/mol and Chatterjee et al. [40] 113 kJ/mol. The reason for the difference might be the use of different rate expressions and in addition there is no information about which ion is used in the zeolite in the work by Chatterjee et al. [40]. The activation energies for the standard SCR reaction over vanadia are in the comparable range; 99 kJ/mol according to Willi et al. [31] and 67 kJ/mol according to Lietti et al. [35].

4.5. Validation

The kinetic model described in the previous sections was validated with six separate experiments, which were not included in the model development and parameter fitting. In the first experiment was the catalyst exposed to 500 ppm NO, 8% O_2, 5% H_2O and variable NH_3 concentration levels (200, 300, 400, 500, 600, 700 and 800 ppm NH_3) at 175 °C. The resulting concentrations of NO, NO_2, NH_3 and N_2O are shown in Fig. 9. Initially, only 200 ppm NH_3 is added to the feed and the conversion of NO is, therefore, low. The conversion gradually increases with time and this is in the model described by a build up of the ammonia on the active sites. The SCR reaction depends on the coverage of ammonia on the surface and the rate, therefore, increases when the ammonia storage increases. In the next two following steps 300 and 400 ppm of NH_3, respectively, are added. A slow increase of conversion is observed, due to that the catalyst is not yet fully saturated with ammonia. At 500 ppm NH_3 steady-state is observed and ammonia also starts to break through. Increasing the ammonia concentration further does result in a higher ammonia slip. In addition, the NO conversion rate decreases slightly. This is due to an ammonia blocking effect, which we previously have observed [16] and also verified with FTIR [17]. This is also

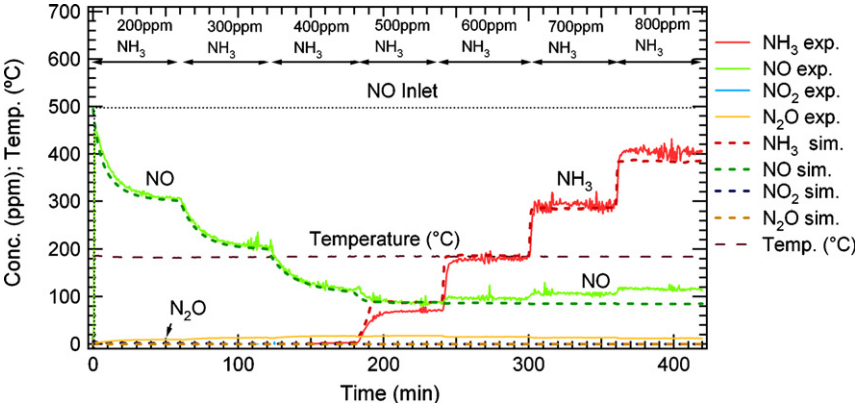

Fig. 9. Measured and calculated concentrations during NH_3 SCR experiment at 175 °C. The feed contained 500 ppm NO, 8% O_2 while varying the NH_3 concentration (200, 300, 400, 500, 600, 700 and 800 ppm). The temperature shown is measured in the centre of the catalyst. The total flow rate is 3500 ml/min.

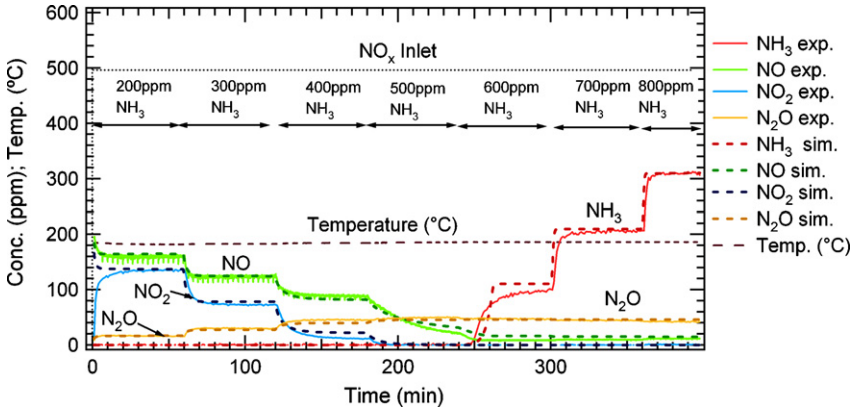

Fig. 10. Measured and calculated concentrations during NH_3 SCR experiment at 175 °C, when varying the NH_3 concentration (200, 300, 400, 500, 600, 700 and 800 ppm NH_3) and using 250 ppm NO, 250 ppm NO_2, 8% O_2, 5% H_2O. The temperature shown is measured in the centre of the catalyst. The total flow rate is 3500 ml/min.

observed for vanadia-based catalysts and Tronconi et al. [13] propose a term for the inhibition in their rate expression. Our model describes the inhibition at higher NH_3 concentrations and predicts a constant NO level. This occurs because at 500 ppm ammonia our catalyst is saturated with NH_3 and increasing the concentration does not increase the surface coverage. Thus, this results in the same SCR rate. The inhibition term developed by Tronconi et al. [13] was investigated, but since our catalyst is saturated and the ammonia coverage is constant this did not give any extra information. The differences between the catalysts are likely the way they adsorb the ammonia. The increase in NO when increasing the ammonia concentration with 100 ppm is only 10 ppm for our catalyst. Thus our model can describe the NO levels out from the catalyst well.

In the second experiment equimolar amounts of NO and NO_2 were used (250 ppm NO and 250 ppm NO_2), 8% O_2, 5% H_2O and variable ammonia concentration levels in the same way as described for the previous experiment (200, 300, 400, 500, 600, 700 and 800 ppm NH_3). The results are shown in Fig. 10. Initially 200 ppm NH_3 is added to the feed and the concentration of NO in the outlet feed is 160 ppm, NO_2 135 ppm and N_2O 15 ppm. The rapid SCR reaction dominates when using equimolar amounts of NO and NO_2. The reason for the lower concentration of NO_2 compared to NO is the production of N_2O from the NO_2. The stoichiometry between N_2O produced and NO_2 consumed is 1:2, which means that to produce 15ppm N_2O; 30 ppm NO_2 is needed. The difference between the NO_2 and NO experimentally is 25 ppm because some of the NO reacts through the standard SCR route. This is more evident for the case where 400 ppm NH_3 is used. In this case 46 ppm N_2O is produced, which corresponds to a consumption of 92 ppm NO_2, but the difference between NO_2 and NO is only 76 ppm. The model describes the levels very well, which indicates that the proposed stoichiometry in the N_2O reaction is valid. When increasing the ammonia concentration the NO_x emitted decreases and N_2O increases simultaneously. With 600 ppm NH_3 in the inlet feed the ammonia is observed breaking through and the ammonia concentration out of the catalyst increases gradually when the inlet NH_3 is increased further; however, the NO and N_2O levels remain constant. The model describes this adequately because the catalyst is saturated with ammonia and the coverage of ammonia does not increase when the NH_3 concentration is increased in the inlet feed.

The model was also validated with short transient experiments, which were not included in the model development and fitting of the parameters. In the first two experiments Cat. 1b was used and the temperature was 350 °C. The catalyst was initially exposed to 500 ppm NO, 500 ppm NH_3, 8% O_2 and 5% H_2O. This was followed by adding different concentrations of NO_2 to the gas mixtures in 2 min pulses. The corresponding NO addition was added to a gas mixture containing 500 ppm NO_2, 500 ppm NH_3, 8% O_2 and 5% H_2O. The inlet concentrations are shown in Fig. 11, together with the experimental concentrations and the levels predicted by the model. The catalyst reached steady-state very rapid and so the first 40 min of the experiment are not shown in order to display the transients more clearly. In addition, this is the same condition as shown in Fig. 8. In the first pulse is 100 ppm NO_2 added. However, the NO_2 level remains almost constant and instead the NO concentration increases significantly. This is because the rapid SCR reaction between NO, NO_2 and NH_3 occurs first and so there is not enough NH_3 to reduce all of the NO. The model describes this feature successfully. In the third pulse the NO_2 is increased to 300 ppm and in this case NO_2 breaks through which also is well described by the model. There is still a much higher NO concentration compared to NO_2 in the outlet, due to the rapid SCR reaction previously described. When starting the NO_2 SCR period (500 ppm NO_2, 500 ppm NH_3, 8% O_2 and 5% H_2O) there is significantly more NO_x in the outlet, in the form of NO_2. This is due to the slow NO_2 SCR reaction. In addition, significant amounts of N_2O are formed. The model describes this well and N_2O in the model is formed by a reaction with NO_2. When adding NO to the gas mixture the N_2O decreases and simultaneously the NO_2 concentration increases. The increase in NO concentration in the outlet is very small for the 100 and 200 ppm pulses and only reaches about 80 ppm for the addition of 300 ppm NO. The reason for this behavior is likely the same as we suggested for

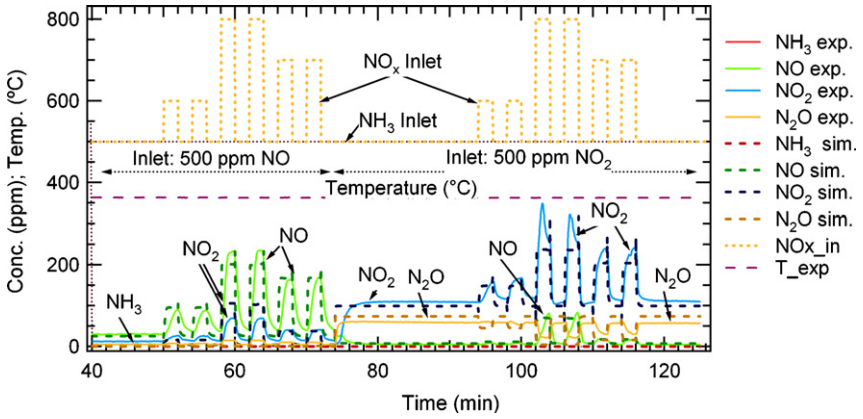

Fig. 11. Inlet, measured and calculated concentrations during NO and NO_2 transient experiment at 350 °C. The temperature shown is measured in the centre of the catalyst. The total flow rate is 3500 ml/min. Cat. 1b is used.

the NO_2 pulses; when adding NO the rapid SCR reaction occurs ($NO + NO_2 + NH_3$) and there is less NH_3 available for the slow NO_2 SCR reaction, resulting in an increase in NO_2 in the outlet. Further, there will also be less NH_3 available for the reaction where N_2O is produced which explains the observed decrease in N_2O. The whole experiment is adequately described by the model.

In the second transient experiment the catalyst was first exposed to 500 ppm NO, 500 ppm NH_3, 8% O_2 and 5% H_2O. This was followed by adding different amounts of NO_2 to the inlet gas mixture, while keeping the total NO_x and NH_3 constant at 500 ppm. The inlet levels and results from the experiment and the model are shown in Fig. 12. Only the transient part of the experiment is shown, because steady-state was reached very rapid. The model can also describe this experiment well. In the first two pulses the NO_2 content is 20% and this results in an increased conversion due to the rapid SCR reaction, between NO, NO_2 and NH_3. In the following two pulses NO_2 is the only NO_x source and here the NO_x concentration increases significantly because the NO_2 SCR reaction is slower than both the rapid SCR and standard SCR reaction. In the simulation the NO_2 concentration reaches steady-state faster than in the experiment. This is likely due to the formation of nitrates on the surface, which we have observed with FTIR [17]. This was not added to the model, in order to make the model as simple as possible. In addition, the amount of NO_x adsorbed on the catalyst is much smaller compared to the ammonia storage. The significance of the ammonia storage is shown in Fig. 6, where an ammonia SCR experiment at 175 °C is shown. The total uptake of ammonia was 12 min and the time before steady-state was approximately 23 min. Further, when increasing the amount of NO_2 (Fig. 12) the N_2O production is also increased in the same way as described above.

In the last two validation experiments another, shorter (15 mm) catalyst sample (Cat. 2) was used which was found to have higher NH_3 storage and activity. The reason might be that these experiments were among the first on this sample, thus no deactivation had occurred. The number of sites was, therefore, fitted to the two experiments described below, resulting in 318.4 mol-sites/m^3 monolith. All kinetic parameters were remained constant in the simulations. The inlet concentration of O_2 was 8%, H_2O 5% and the NO and NH_3 concentrations were varied. The inlet values for NO and NH_3 are plotted in Figs. 13 and 14. The results from the experiments and simulations at 175 and 350 °C are also shown in Figs. 13 and 14, respectively. In the initial part of the experiment at 175 °C we observe the effects of the ammonia storage, which is described together with Fig. 7. After 50 min the NO transients

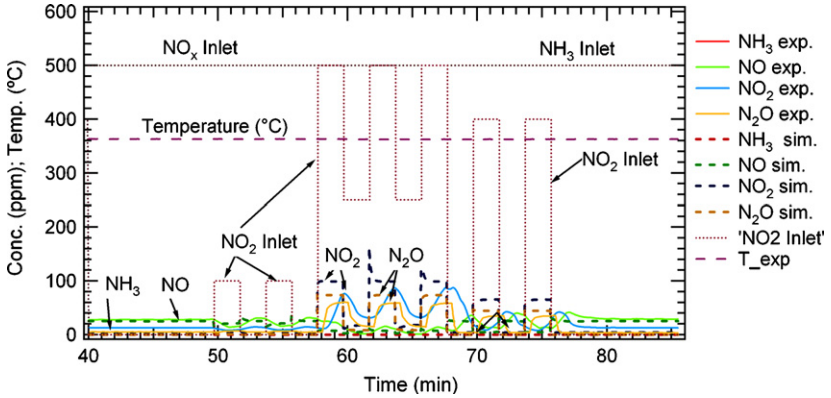

Fig. 12. Inlet, measured and calculated concentrations during NO and NO_2 transient experiment at 350 °C. The temperature shown is measured in the centre of the catalyst. The total flow rate is 3500 ml/min. Cat. 1b is used.

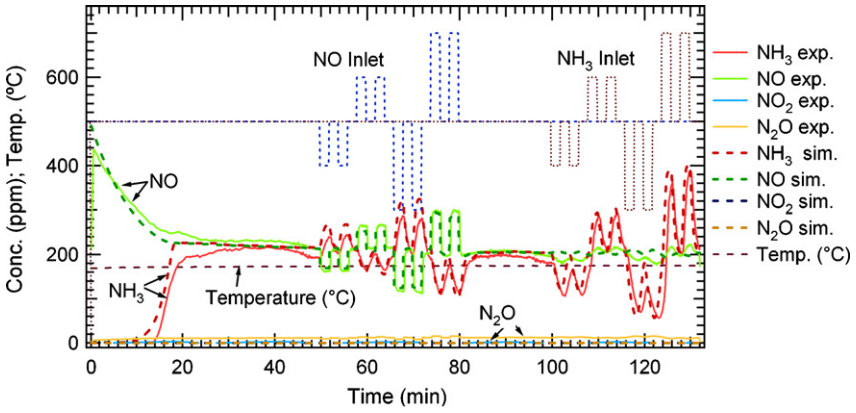

Fig. 13. Inlet, measured and calculated concentrations during NO and NH_3 transient experiment at 175 °C. The temperature shown is measured in the centre of the catalyst. The total flow rate is 3500 ml/min. Cat. 2 is used.

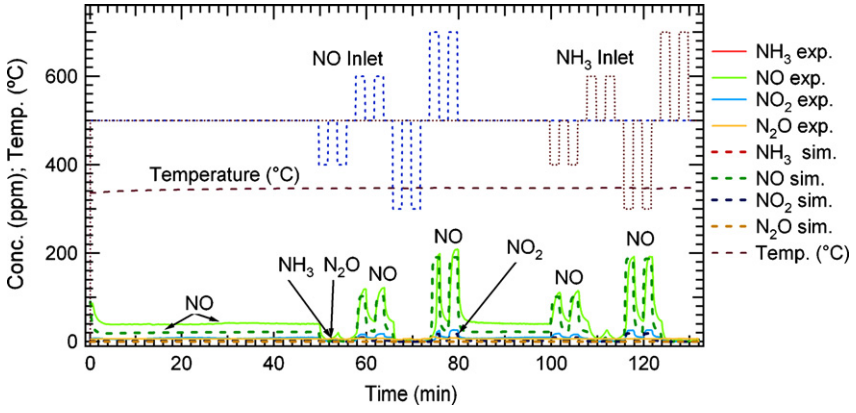

Fig. 14. Inlet, measured and calculated concentrations during NO and NH_3 transient experiment at 350 °C. The temperature shown is measured in the centre of the catalyst. The total flow rate is 3500 ml/min. Cat. 2 is used.

are started and it can be observed that when the NO decreases at the inlet, the NO emissions from the catalyst also decrease and the opposite occurs when the NO increases at the inlet. However, for the ammonia transients the NO conversion is almost constant, due to the large ammonia storage on the catalyst. Thus the coverage of ammonia on the surface is similar during the 2 min transients. It can also be observed that the ammonia out does not reach steady-state during the 2 min which is also due to the large ammonia adsorption on the catalyst. In Fig. 14, the results from the corresponding experiment at 350 °C are presented which show that when the NO concentration decreases the conversion of NO increases. The opposite occurs when the NO is increased in the inlet feed. The ammonia emissions from the catalyst are zero during the whole experiment because of the rapid NH_3 oxidation. In addition, when the ammonia concentration changes the NO concentration changes immediately. However, at 175 °C the NO conversion was almost constant, when changing the ammonia concentration. At 350 °C there is low storage of ammonia because of the rapid NH_3 oxidation, which causes the rapid changes of NO emissions when changing the NH_3. In our FTIR study [17] we observed high concentrations of ammonia on the surface at 175 °C, but at 350 °C very low amounts were found, which supports the results from our model.

5. Conclusions

The activity of Cu-ZSM-5 for NH_3 SCR was investigated using flow reactor experiments and kinetic modeling. The mass-transfer in the wash-coat was first studied. This was done by using two catalyst samples with different wash-coat amounts (Cat. 2: 496 mg zeolite, Cat. 3: 265 mg zeolite). The total feed flow rate was doubled for the sample which had double the mass of zeolite, so that the same flow rate per gram zeolite was obtained. The ammonia and nitrogen oxide conversions were observed to be essentially the same for the whole experiment, where the temperature was increased in steps from 100 to 500 °C. At higher temperatures (300 °C and above) it is difficult to draw conclusions regarding mass-transfer since the conversion of ammonia is close to 100%. However, at temperatures below 300 °C the results show that there are no mass-transfer limitations in the wash-coat for the standard SCR reaction.

The kinetic model was developed using a broad range of experimental conditions. In all experiments 5% water was used because it influences the amount of ammonia stored and the SCR activity of the catalyst. For describing transient experiments it is crucial to have a good description of the amount of ammonia adsorbed on the catalyst, and therefore, one NH_3 TPD experiment was used to estimate the parameters for ammonia adsorption and desorption. The ammonia

desorption occurred over a broad temperature interval, thus ammonia is adsorbed with different energies on the surface. It is likely that it adsorbs on different sites in the catalyst. In order to make the model as simple as possible only one site was used and the activation energy for the desorption is coverage dependent. The NO oxidation was simulated as a reversible reaction step using results from one variable-temperature experiment with NO, O_2 and H_2O in the feed. At low temperatures the conversion was kinetically limited and at 500 °C determined by thermodynamic restrictions. The model included steps for the NH_3 oxidation, standard SCR ($NO + O_2 + NH_3$), rapid SCR ($NO + NO_2 + NH_3$), NO_2 SCR ($NO_2 + NH_3$) and N_2O formation, and the parameters were estimated by fitting to four experiments: one NH_3 oxidation experiment and one SCR experiment where the temperature was increased stepwise from 100 to 500 °C, and two experiments where the NO-to-NO_2 ratio was varied. There is a large storage of ammonia initially in the SCR experiment, resulting in a total uptake of about 15 min. The conversion increases and is close to 100% by 200 °C. However, at 350 °C the conversion starts to decrease due to rapid ammonia oxidation. The experiments with a changing NO_2-to-NO_x ratio showed that the maximum conversion occurs at about 50% NO_2. In addition for most cases the amount of N_2O increased when increasing the NO_2. The kinetic parameters and 95% linearized confidence intervals are given in the paper. The model describes all experiments well.

The model was validated with six separate experiments not included in the kinetic parameter estimation. In the first experiment the inlet feed gas consisted of 500 ppm NO, 8% O_2, 5% H_2O and the ammonia concentration was varied from 200 up to 800 ppm at 175 °C. When increasing the ammonia concentration the NO conversion increased gradually up to 500 ppm ammonia in the inlet feed. At each step the NO concentration was changed quite slowly, due to the slow increase in ammonia coverage on the surface. At higher ammonia levels ammonia inhibition was observed. In the second experiment the NO_x source was changed from NO only to a 50% mixture of NO and NO_2. In this experiment the interplay between the reactions for standard SCR and rapid SCR as well as N_2O production was observed. The last four experiments used for validating the model were short transient experiments where the NO, NH_3 and NO_2 concentrations were varied stepwise with duration of 2 min for each step. Interestingly, when adding 100 ppm NO_2 to the feed, which consisted of 500 ppm NO, 500 ppm NH_3 and 5 % H_2O, an increase of the NO emissions was observed from the catalyst because the rapid SCR reactions occurs consuming the NO_2 and consequently there is less ammonia available for the standard SCR reaction. In the NH_3 transients at 175 °C the ammonia out does not reach steady-state during the 2 min, due to the large ammonia storage. Because of the large amount of ammonia in the catalyst, the conversion of NO is almost constant. However, at 350 °C the NO conversion is very sensitive to the amount of NH_3 in the transients because at this high temperature the ammonia oxidation is rapid and the coverage of ammonia is low which is confirmed by FTIR measurements. The model describes all six-validation experiments well.

Acknowledgements

The work is performed at Competence Centre for Catalysis (KCK), Chalmers and at General Motors Research and Development Center. The authors would like to acknowledge helpful discussions with Se Oh, Ed Bissett, Jong-Hwan Lee, Byong Cho and Steven J. Schmieg of the General Motors Research and Development Center and Ashok Gopinath at GM ISL. We would also like to acknowledge Ed Bissett for the GM fortran code for emission control simulations, which has been used in this work. We would also like to thank GM R&D Center for the financial support. One author (Louise Olsson) would also like to acknowledge the Swedish Research Council (Contract: 621-2003-4149 and 621-2006-3706) for additional support.

References

[1] A. Fritz, V. Pitchon, Appl. Catal. B 13 (1997) 1.
[2] R.M. Heck, R.J. Farrauto, Appl. Catal. A 221 (2001) 443.
[3] L. Olsson, R.J. Blint, E. Fridell, Ind. Eng. Chem. Res. 44 (9) (2005) 3021.
[4] L. Olsson, D. Monroe, R.J. Blint, Ind. Eng. Chem. Res. 45 (26) (2006) 8883.
[5] R. Burch, J.P. Breen, C.J. Hill, B. Krutzsch, B. Konrad, E. Jobson, L. Cider, K. Eranen, F. Klingstedt, L.E. Lindfors, Appl. Catal. B: Environ. 13 (1) (1997) 12.
[6] H.Y. Chen, W.M.H. Sachtler, Catal. Today 42 (1–2) (1998) 18.
[7] M. Koebel, M. Elsener, M. Kleeman, Catal. Today 59 (3–4) (2000) 335.
[8] M. Kleeman, M. Elsener, M. Koebel, A. Wokaun, Ind. Eng. Chem. Res. 39 (2000) 4120.
[9] N.-Y. Topsoe, H. Topsoe, J.A. Dumesic, J. Catal. 151 (1995) 226.
[10] J.A. Dumesic, N.-Y. Topsoe, H. Topsoe, Y. Chen, T. Slabiak, J. Catal. 163 (1996) 409.
[11] I.E. Wachs, G. Deo, B.M. Weckhuysen, A. Andreini, M.A. Vuurman, M. de Boer, D.D. Amiridis, J. Catal. 161 (1996) 211.
[12] B. Roduit, A. Wokaun, A. Baiker, Ind. Eng. Chem. Res. 37 (1998) 4577.
[13] E. Tronconi, I. Nova, C. Ciardelli, D. Chatterjee, B. Bandl-Konrad, T. Burkhardt, Catal. Today 105 (2005) 529.
[14] C. Ciardelli, I. Nova, E. Tronconi, D. Chatterjee, B. Bandl-Konrad, M. Weibel, B. Krutzsch, Appl. Catal. B: Environ. 70 (2007) 80.
[15] E. Tronconi, I. Nova, C. Ciardelli, D. Chatterjee, M. Weibel, J. Catal. 245 (2007) 1.
[16] H. Sjövall, L. Olsson, E. Fridell, R.J. Blint, Appl. Catal. B: Environ. 64 (2006) 180.
[17] H. Sjövall, E. Fridell, R.J. Blint, L. Olsson, Top. Catal. 42–43 (1–4) (2007) 113.
[18] J.H. Park, H.J. Park, J.H. Baik, I.-S. Nam, C.-H. Shin, J.H. Lee, B.K. Cho, S.H. Oh, J. Catal. 240 (2006) 47.
[19] K. Rahkamaa-Tolonen, T. Manula, M. Lomma, M. Huuhtanen, R.L. Keiski, Catal. Today 100 (2005) 217.
[20] J.H. Baik, S.D. Yim, I.-S. Nam, Y.S. Mok, J.H. Lee, B.K. Cho, S.H. Oh, Ind. Eng. Chem. Res. 45 (2006) 5258.
[21] G. Delahay, S. Kieger, N. Tanchoux, P. Trens, B. Coq, Appl. Catal. B: Environ. 52 (2004) 251.
[22] S. Kieger, G. Delahay, B. Coq, B. Neveu, J. Catal. 183 (1999) 267.
[23] S. Stevenson, J.C. Vartuli, C.F. Brooks, J. Catal. 190 (2000) 228.
[24] J. Eng, H. Bartholomew, J. Catal. 171 (1997) 27.
[25] M. Devadas, O. Kröcher, M. Elsener, A. Wokaun, N. Söger, M. Pfeifer, Y. Demel, L.L. Mussman, Appl. Catal. B: Environ. 67 (2006) 187.
[26] O. Kröcher, M. Devadas, M. Elsener, A. Wokaun, N. Söger, M. Pfeifer, Y. Demel, L. Mussman, Appl. Catal. B: Environ. 66 (2006) 208.

[27] B. Coq, M. Mauvezin, G. Delahay, J.B. Butet, S. Kieger, S. Appl. Catal. B: Environ. 27 (2000) 193.
[28] M. Koebel, G. Madia, M. Elsener, Catal. Today 73 (3–4) (2002) 239.
[29] D. Chatterjee, T. Burkhardt, M. Weibel, E. Tronconi, I. Nova, C. Ciardelli, SAE paper 2006-01-0468, 2006.
[30] P. Forzatti, Appl. Catal. A 222 (2001) 221.
[31] R. Willi, B. Roduit, R.A. Koeppel, A. Wokaun, A. Baiker, Chem. Eng. Sci. 51 (11) (1996) 2897.
[32] R. Willi, M. Maciejewski, U. Gobel, R.A. Köppel, A. Baiker, J. Catal. 166 (1997) 356.
[33] C. Winkler, P. Forchinger, P. Patil, J. Gieshoff, P. Spurk, M. Pfeifer, SAE Paper 2003-01-0845, 2003.
[34] J.C. Wurzenberger, R. Wanker, SAE-paper 2005-01-0948, 2005.
[35] L. Lietti, I. Nova, E. Tronconi, P. Forzatti, Catal. Today 45 (1998) 85.
[36] H.J. Chae, S.T. Choo, H. Choi, I.S. Nam, H.S. Yang, S.L. Song, Ind. Eng. Chem. Res. 39 (2000) 1159.
[37] E. Tronconi, A. Cavanna, P. Forzatti, Ind. Eng. Chem. Res. 37 (1998) 2341.
[38] V. Tomasic, Z. Gomzi, S. Zrncevic, React. Kinet. Lett. 77 (2002) 245.
[39] S. Malmberg, M. Votsmeier, J. Gieshoff, N. Söger, L. Mußmann, A. Schuler, A. Drochner, Top. Catal. 42–43 (2007) 33.
[40] D. Chatterjee, T. Burkhardt, M. Weibel, I. Nova, A. Grossale, E. Tronconi, SAE paper 2007-01-1136, 2007.
[41] S.P. Felix, C. Savill-Jowitt, D.R. Brown, Thermochim. Acta 433 (2005) 59.
[42] T. Komatsu, M. Nunokawa, I.S. Moon, T. Takahara, S. Namba, T. Yashima, Catal. J. 148 (1994) 427.